Model for Calculating Photosynthetic Photon Flux Densities in Forest Openings on Slopes

JING M. CHEN AND T. ANDREW BLACK

Department of Soil Science, University of British Columbia, Vancouver, British Columbia, Canada

DAVID T. PRICE

Northern Forestry Centre, Forestry Canada, Edmonton, Alberta, Canada

REID E. CARTER

Remtech Group, Vancouver, British Columbia, Canada

(Manuscript received 20 October 1992, in final form 15 March 1993)

ABSTRACT

A model has been developed to calculate the spatial distribution of the photosynthetic photon flux density (PPFD) in elliptical forest openings of given slopes and orientations. The PPFD is separated into direct and diffuse components. The direct component is calculated according to the opening and radiation geometries, and pathlength of the solar beam through the forest canopy. The diffuse component is obtained from the sky, tree, and landscape view factors. In this model, the distribution of foliage area with height and the effect of foliage clumping on both direct and diffuse radiation transmission are considered.

The model has been verified using measurements from six quantum sensors (LI-COR Inc.) located at different positions in a small clear-cut (0.37 ha) in a 90-year-old western hemlock–Douglas fir forest.

1. Introduction

Clear-cutting has been the major timber-harvesting method in the forest industry in British Columbia. Forest regeneration in clear-cuts has been a controversial issue causing considerable public and scientific concern. As clear-cut size increases, the disturbance to a forest ecosystem increases as does the harshness of the microclimate for the survival and growth of tree seedlings, especially for clear-cuts in high elevation or dry regions. The felling of small groups of trees in a forest stand (group selection) is being considered as one of the alternatives for timber harvesting. This method has the advantage of low disturbance. Geiger (1966) reported results of studies showing increasing daytime and decreasing nighttime air temperature near the surface at the center of forest clearings as clearing size increased from 0 to 80 m in diameter. However, there has not been enough quantitative information on the microclimate in openings of various sizes to provide justification for the choice of alternative silvicultural systems. Photosynthetically active radiation (PAR) is one of the important components of the microclimate critical for forest regeneration. The purpose of this paper is (i) to describe a model developed for calculating photosynthetic photon flux density (PPFD), a measure of the flux of PAR, at given positions in forest openings of various sizes and shapes on surfaces of various slopes and orientations; and (ii) to report the results of experimental tests of the model carried out in a small clear-cut on a forested slope.

There have been several published studies of radiation in forest clear-cuts. Holbo and Childs (1987) measured radiation budgets in six forest clear-cuts of various sizes, slopes, and aspects. The measured components included the downward and upward shortwave and longwave radiation fluxes. Harrington (1984) provided a computer algorithm for calculating the solar irradiance in strip clear-cuts on sloping surfaces, where the solar irradiance above the stand was separated into direct and diffuse components. In his model, the clear-cut sides were treated as two parallel impenetrable walls for direct and diffuse radiation, and diffuse radiation from the sky was considered to be the only source of diffuse radiation in the clear-cut.

The model presented here extends the previous work in several respects. First, the geometry of the opening is elliptical. By varying the lengths of the axes of the ellipse, the geometry of forest openings of a wide range of sizes and shapes can be described. For example, strip clear-cuts can be approximated in the model by setting one axis of the ellipse to be much longer than the other. Second, the new model considers all the major transfer mechanisms for diffuse PPFD. In forest openings, es-

Corresponding author address: Dr. Jing M. Chen, Global Monitoring Section, Canada Centre for Remote Sensing, 588 Booth Street (4th Floor), Ottawa, Ontario, K1A 0Y7, Canada.

pecially in small openings resulting from group selection cutting, the diffuse component may account for more than half the total PPFD incident at the forest floor. The diffuse PPFD not only originates from the sky but also results from several other radiation transfer mechanisms including the transmission of PAR from the sky through the canopy, scattering of direct and diffuse PAR by the foliage, and the reflection of the incident PAR from the surrounding forest edges. Third, the model calculates not only the direct PAR coming over the tops of the trees but also that transmitted through the forest. In small openings and at positions near forest edges, the solar beam transmitted through the forest canopy is an important source of PAR.

2. Theory

a. Opening geometry

Figure 1 shows a schematic diagram of an elliptical opening on an extensive surface that can be assigned any slope (zenith angle θ_s) from 0° to 90° and aspect (azimuthal angle β_s) from 0° to 360°. By mathematical convention, the angle β_s increases counterclockwise from the x axis. This makes north 0°, west 90°, south 180°, and east 270° when the x axis is pointed to the north. The ellipse can be rotated to obtain a desired angle of one of the axes with respect to the maximum elevation gradient of the surface. No matter how the opening is rotated, oriented, and inclined, the trees are always vertical.

Figure 2 shows the opening as viewed vertically from above. The surface of the opening is thus projected onto a horizontal plane. Since the trees are always vertical, it is more straightforward to do calculations using a horizontal coordinate system than using a system defined by the slope. The diagonal straight line across the ellipse represents the direction of either the solar beam or a ray of skylight. For the calculation of direct and diffuse PPFD at a point (X_0, Y_0) on the inclined opening surface corresponding to the projected point (x_0, y_0) on a horizontal plane (see Fig. 3), it is essential to know the incidence angles of the treetops at the two intercepting points (x_1, y_1) and (x_2, y_2). These two points in the horizontal coordinate system can be obtained by solving the following two equations,

$$y - y_0 = \tan\beta(x - x_0) \tag{1}$$

$$\frac{x^2}{a_p^2} + \frac{y^2}{b_p^2} = 1, \tag{2}$$

where a_p and b_p are the lengths of the axes of the ellipse (in the x and y axis directions, respectively) projected on a horizontal surface and β is the azimuthal angle of the ray. These two points are therefore obtained as follows:

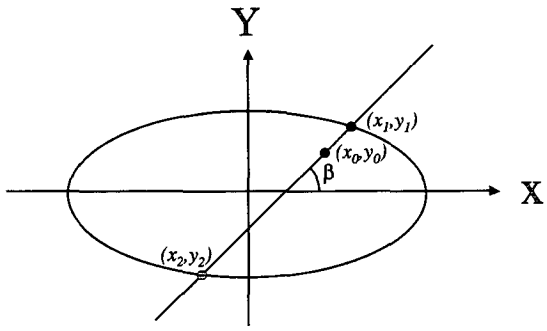

FIG. 2. An ellipse on a slope projected on the horizontal x–y plane, where (x_0, y_0) is the projected point of interest and (x_1, y_1) and (x_2, y_2) are the two points intercepted by a straight line through (x_0, y_0) in the direction β.

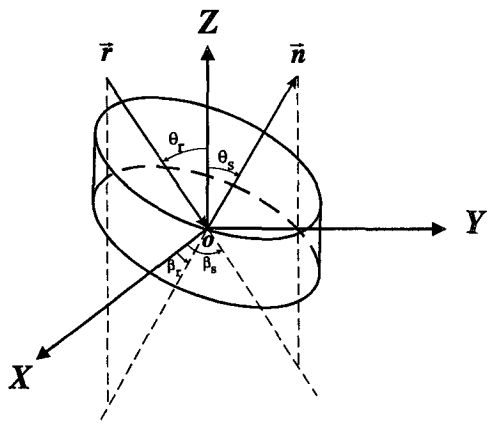

FIG. 1. The coordinates and vectors for a sloping forest opening; **n** is the normal to the opening surface with a zenith angle θ_s (slope) and an azimuth angle β_s (aspect), and **r** represents the direction of the solar beam or a ray of skylight with a zenith angle θ_r and an azimuth angle β_r. The upper ellipse represents the opening at the treetops.

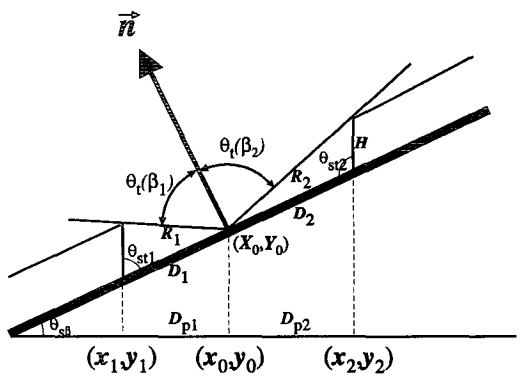

FIG. 3. The incidence angle of treetops, $\theta_t(\beta_1)$ and $\theta_t(\beta_2)$, for the location (X_0, Y_0) in the opening, where β_1 and β_2 are in opposite directions (180° apart); $\theta_{s\beta}$ is the slope in the direction β; and R_1, R_2, D_1, D_2, D_{p1}, and D_{p2} are distances for the labeled line segments, respectively. For example, R_1 is the distance between (X_0, Y_0) and the treetops at the lower edge of the opening.

$$x_1 = \frac{-B + (B^2 - 4AC)^{1/2}}{2A},$$

$$y_1 = y_0 + \tan\beta(x_1 - x_0) \quad (3)$$

$$x_2 = \frac{-B - (B^2 - 4AC)^{1/2}}{2A},$$

$$y_2 = y_0 + \tan\beta(x_2 - x_0), \quad (4)$$

where

$$A = a_p^2 \tan\beta + b_p^2 \quad (5)$$

$$B = 2a_p^2(y_0 \tan\beta - x_0 \tan^2\beta) \quad (6)$$

$$C = a_p^2 y_0^2 - 2a_p^2 x_0 y_0 \tan\beta + a_p^2 \tan^2\beta x_0^2 - a_p^2 b_p^2. \quad (7)$$

The projected axes a_p and b_p are related to the axes of the ellipse on the sloping surface, a and b, by

$$a_p = a \cos\theta_{p1} \quad (8)$$

$$b_p = b \cos\theta_{p2}, \quad (9)$$

where

$$\theta_{p1} = \arctan(\cos\Delta\beta \tan\theta_s) \quad (10)$$

$$\theta_{p2} = \arctan\left[\cos\left(\Delta\beta + \frac{\pi}{2}\right)\tan\theta_s\right], \quad (11)$$

where $\Delta\beta$ is the difference between the azimuthal direction of axis $a(\beta_a)$ and the aspect of the normal to the opening surface β_s (i.e., $\beta_a - \beta_s$).

When the points (x_1, y_1) and (x_2, y_2) are known, the maximum incidence angles $[\theta_t(\beta_1)$ and $\theta_t(\beta_2)]$ of a beam or a ray not intercepted by the treetops at these two points can be calculated (Fig. 3). An incidence angle is defined as the angle between the direction of incidence to a point and the normal to the surface at that point; $\theta_{s\beta}$ is the slope in the direction β and is calculated from (see appendix A)

$$\theta_{s\beta} = \arctan[\tan\theta_s \cos(\beta - \beta_s)]. \quad (12)$$

The angles between the vertical trees and the slope line in the direction β at (x_1, y_1) and (x_2, y_2) are θ_{st1} and θ_{st2}, respectively, and are simply as follows,

$$\theta_{st1} = \frac{\pi}{2} - \theta_{s\beta} \quad (13)$$

$$\theta_{st2} = \frac{\pi}{2} + \theta_{s\beta}. \quad (14)$$

The distances D_1 and D_2 in Fig. 3 are obtained from

$$D_1 = \frac{D_{P1}}{\cos\theta_{s\beta}} \quad (15)$$

$$D_2 = \frac{D_{P2}}{\cos\theta_{s\beta}}, \quad (16)$$

where D_{p1} and D_{p2} are the distances between (x_1, y_1) and (x_0, y_0) and between (x_2, y_2) and (x_0, y_0), respectively, given by

$$D_{p1} = [(x_1 - x_0)^2 + (y_1 - y_0)^2]^{1/2} \quad (17)$$

$$D_{p2} = [(x_2 - x_0)^2 + (y_2 - y_0)^2]^{1/2}. \quad (18)$$

The incidence angles $\theta_t(\beta_1)$ and $\theta_t(\beta_2)$ can then be calculated using the sine theorem as follows:

$$\frac{1}{H}\sin\left[\frac{\pi}{2} - \theta_t(\beta_1)\right] = \frac{\sin\theta_{st1}}{R_1} \quad (19)$$

$$\frac{1}{H}\sin\left[\frac{\pi}{2} - \theta_t(\beta_2)\right] = \frac{\sin\theta_{st2}}{R_2}, \quad (20)$$

where H is the average tree height, and R_1 and R_2 are obtained from the cosine theorem as follows,

$$R_1 = (D_1^2 + H^2 - 2HD_1 \cos\theta_{st1})^{1/2} \quad (21)$$

$$R_2 = (D_2^2 + H^2 - 2HD_2 \cos\theta_{st2})^{1/2}. \quad (22)$$

b. PPFD on a sloping surface

1) DIRECT PPFD

(i) *Direct PPFD over the tops of the trees*

The boundary of the opening is treated as a wall with an average tree height H. If the solar beam travels over the wall to the point (X_0, Y_0) in the opening, that is, the solar incidence angle at that point is smaller than the maximum incidence angle determined by the treetops in the sun's direction $[\theta_t(\beta)]$, the direct PPFD at that point (Q_{Ds}) is calculated from the projection of the vector representing the beam to the normal to the surface, that is,

$$Q_{Ds} = Q_{Dp}[\cos\theta_r \cos\theta_s + \sin\theta_r \sin\theta_s \cos(\beta_r - \beta_s)], \quad (23)$$

where θ_r and β_r are the sun's zenith and azimuth angle, respectively, and Q_{Dp} is the unattenuated direct PPFD on a surface perpendicular to the direction of the solar beam calculated from

$$Q_{Dp} = \frac{Q_D}{\cos\theta_r}, \quad (24)$$

where Q_D is the direct PPFD on a horizontal surface as measured by a horizontally positioned quantum sensor.

The solar zenith and azimuth angles are calculated as functions of longitude, latitude, the day of the year, and the time of day using equations given in Gates (1980). The equation of time is included in the calculations of local solar time.

(ii) *Direct PPFD transmitted through the forest*

When the solar incidence angle is larger than $\theta_t(\beta)$, the solar beam is attenuated by the surrounding trees. Figure 4 shows how the attenuation is considered. The

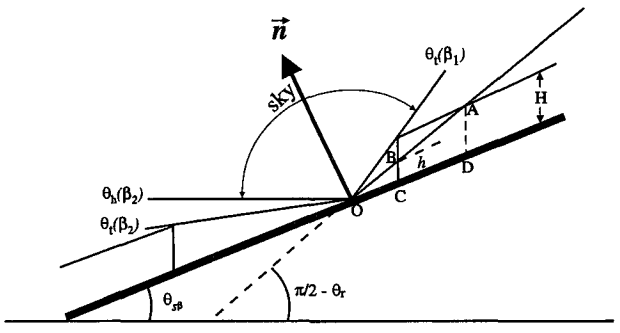

FIG. 4. Schematic diagram showing the sky, tree, and landscape view factors, and the path $\overline{AB}$ of the solar beam passing through the forest in the direction β_1 and at a zenith angle θ_r to the point O [i.e., (X_0, Y_0)] on the ground in the opening; h is the exit height of the beam.

path of the beam through the canopy from point A to B can be calculated from several previously defined terms using the following equation (see appendix B):

$$\overline{AB} = \cos\theta_{s\beta}\left[\frac{H}{\cos(\theta_r + \theta_{s\beta})} - \frac{D_2}{\sin\theta_r}\right]. \quad (25)$$

In the case that the sun is in the downslope direction, the path $\overline{AB}$ can still be calculated with Eq. (25) except that D_2 is replaced with D_1 and the sign of $\theta_{s\beta}$ becomes negative.

Most coniferous canopies do not have a uniform distribution of leaf area with height. It has been assumed that the leaf area density increases linearly with depth into the canopy to one third of the tree height (see Fig. C1). Below that height is the trunk space, which has a negligible plant (trunk, branch, and leaf) area compared with the leaf area above (see appendix C). The probability P of a solar beam penetrating the canopy along the path $\overline{AB}$ is then calculated as

$$P = \exp[-G(\theta_r)\Omega L_{hp}], \quad (26)$$

where $G(\theta_r)$ is the mean coefficient of projection of a unit leaf area on a plane perpendicular to the direction of the solar beam; Ω is a clumping index depending on the spatial arrangement of the foliage elements, assumed to be 0.5 from our previous work with Douglas fir canopies (Chen et al. 1991; Chen and Black 1991, 1992); L_{hp} is the leaf area index accumulated over the path $\overline{AB}$ derived as (appendix C)

$$L_{hp} = L\overline{AB}\frac{H - h}{(H - H_0)^2}, \quad (27)$$

where L is the leaf area index of the stand, taken to be 9.0, H_0 equals $H/3$, and h is the exit height from the opening edge, which is $\overline{BC}$ in Fig. 4. Since no plant area is assumed below H_0, h is taken to be H_0 when it is less than H_0.

The projection coefficient $G(\theta_r)$ is calculated using the following empirical equation obtained from our previous work in Douglas fir stands (Black et al. 1991),

$$G(\theta_r) = \begin{cases} 0.54 + 0.33\theta_r, & \theta_r < 0.85 \\ 0.82 - 1.14(\theta_r - 0.85), & \theta_r \geq 0.85, \end{cases} \quad (28)$$

where θ_r is in radians. For coniferous species other than Douglas fir, no data are available, and $G(\theta_r)$ is taken to be 0.5 in the model.

The transmitted direct PPFD (Q_{Dt}) is then computed from

$$Q_{Dt} = Q_{Ds}P, \quad (29)$$

where Q_{Ds} is obtained from Eq. (23).

2) DIFFUSE PPFD

The total diffuse PPFD (Q_{ds}) on a sloping surface at any point in the opening arises from several sources. It is calculated using the following equation,

$$Q_{ds} = F_sQ_d + (1 - F_s)Q_d\exp(-G_dL_e) + F_tp_t(0.5Q_D + Q_d) + F_lp_l(Q_D + Q_d), \quad (30)$$

where Q_d is the diffuse PPFD incident on a horizontal surface above the canopy; F_s, F_t, and F_l are the sky, tree, and landscape view factors, respectively; p_t and p_l are the reflection coefficients of the trees and the surrounding landscape to the solar radiation, respectively. The latter were taken to be 6% for conifer leaves and 12% for conifer forest, respectively (Jarvis et al. 1976). The first term on the right-hand side of the equation is the diffuse PPFD coming directly from the sky over the opening boundary; the second term denotes the transmission of PAR from the sky and scattering of direct and diffuse PAR through the canopy; the third term results from the reflection of direct and diffuse PAR by trees at the boundary (Q_D is multiplied by 0.5 under the assumption that half of the opening boundary is sunlit); and the fourth term is the reflection of total incident PAR by the surrounding landscape. The fourth term is significant only when the slope is large enough that some part of the surface in the opening sees the surrounding landscape over the treetops along the lower edge of the opening. In the second term, G_d is an extinction coefficient for diffuse PAR, and L_e is the effective leaf area index, being ΩL (Black et al. (1991); G_d is obtained using the following empirical equation derived from our measurements of direct and diffuse PPFD above and below a Douglas fir stand,

$$G_d = 0.85 - 0.04\frac{Q_D}{Q_d}. \quad (31)$$

The principle of the form of this equation is described in Black et al. (1991).

The definitions of the view factors are

$$F_s = \frac{1}{\pi}\int_0^{2\pi} d\beta \int_0^{\theta_1(\beta)} \cos\theta \sin\theta d\theta \quad (32)$$

$$F_t = \frac{1}{\pi}\int_0^{2\pi} d\beta \int_{\theta_2(\beta)}^{\pi/2} \cos\theta \sin\theta d\theta \quad (33)$$

$$F_l = \frac{1}{\pi}\int_0^{2\pi} d\beta \int_{\theta_1(\beta)}^{\theta_2(\beta)} \cos\theta \sin\theta d\theta, \quad (34)$$

where the limits $\theta_1(\beta)$ and $\theta_2(\beta)$ for the integrals with respect to θ are defined by

$$\theta_1(\beta) = \begin{cases} \theta_t(\beta), & \theta_t(\beta) \leqslant \dfrac{\pi}{2} + \theta_{s\beta} \\ \dfrac{\pi}{2} - |\theta_{s\beta}|, & \theta_t(\beta) > \dfrac{\pi}{2} + \theta_{s\beta} \end{cases} \quad (35)$$

$$\theta_2(\beta) = \theta_t(\beta), \quad (36)$$

where $\theta_{s\beta}$ is the slope of the ground surface in the β direction, being negative in the downslope direction (appendix A). The condition of $\theta_t(\beta) > \pi/2 + \theta_{s\beta}$ occurs when the treetops in the downslope direction β are lower than the point O. The principle used in deriving these view factor equations is demonstrated by Howell (1982).

Physical meanings of the view factors are demonstrated in Fig. 4. In the case that the tops of trees in one direction are lower than the point of interest (O), the sky view occupies the incidence angle range from a horizontal line in that direction to the treetops in the opposite direction, while the landscape view extends from the horizontal line down to the treetops in the former direction. The tree view always extends from the tops to the bases of the trees. Equation (35) sets the upper limit for the sky view and lower limit for the landscape view to the horizontal line when the treetops are lower than the point O. The horizontal line has an incidence angle $\theta_h(\beta) = \pi/2 - |\theta_{s\beta}|$. When the point O is lower than the treetops in both directions, $\theta_1(\beta)$ equals $\theta_t(\beta)$, which automatically sets F_l to zero in Eq. (34). Equations (32)–(34) are discretized at intervals of 5° for θ and 15° for β.

c. *PPFD on a horizontal surface at a slope*

The equations presented above are derived for the case that PPFD is on a sloping surface, that is, a surface parallel to the slope of an opening. The other case of interest in many applications is the PPFD incident on a horizontal surface at a point on a slope, such as the case of a radiometer mounted horizontally a short distance above an extensive sloping surface.

1) DIRECT PPFD

The following equation is used to calculate the direct PPFD on a small horizontal surface placed immediately above an extensive slope (Q_{Dh}) including transmission both over the treetops and through the canopy:

$$Q_{Dh} = \begin{cases} Q_D P, & \dfrac{\pi}{2} - \theta_r > \theta_{s\beta} \\ 0, & \dfrac{\pi}{2} - \theta_r \leqslant \theta_{s\beta}, \end{cases} \quad (37)$$

where the probability P of beam transmission through the forest canopy is defined in Eq. (26). It is the same as that for a sloping surface since the horizontal surface is assumed to be close to the slope. The condition $\pi/2 - \theta_r > \theta_{s\beta}$ means that the sun's elevation is larger than the slope in the β direction.

2) DIFFUSE PPFD

Equations (30), (32), (33), and (34) are also used to calculate the diffuse PPFD incident on a horizontal surface at the slope and to calculate the corresponding view factors, except that the limits for the integrals are redefined as follows,

$$\theta_1(\beta) = \begin{cases} \theta_t(\beta) - \theta_{s\beta}, & \theta_t(\beta) \leqslant \dfrac{\pi}{2} + \theta_{s\beta} \\ \dfrac{\pi}{2}, & \theta_t(\beta) > \dfrac{\pi}{2} + \theta_{s\beta} \end{cases} \quad (38)$$

$$\theta_2(\beta) = \theta_t(\beta) - \theta_{s\beta}. \quad (39)$$

These limits are changed because the normal to the horizontal surface is different from the normal to the slope. For a given direction of a ray from the sky, the angle of incidence at the horizontal surface differs by $\theta_{s\beta}$ (the slope in direction β) from that at the slope, where $\theta_{s\beta}$ can be either positive or negative depending on whether the ray is coming from the upslope or downslope direction. For the horizontal surface, the landscape view factor becomes the ground view factor, that is, the horizontal surface sees the upper part of the clearing rather than the landscape.

3. Field experiment

For the purpose of validating the model, field data were collected in a forest opening at the Research Forest of the University of British Columbia at Haney, British Columbia. The latitude and longitude of the research site are 49°20'N and 122°35'W, respectively. The opening is approximately elliptical (Fig. 5), with short and long axes of 60 and 82 m. The opening is on a fairly extensive 12° slope facing approximately west (azimuth angle 75° counterclockwise from north). The surrounding forest is a mixture of 90-year-old western hemlock (*Tsuga heterophylla*) and Douglas fir (*Pseudotsuga menziesii*) trees with an average height of 38 m.

Six quantum sensors (LI-COR Inc, Lincoln, Nebraska, Model LI-190SB) were mounted horizontally about 1 m above the ground at the six locations in the opening shown in Fig. 5. These sensors have an accurate photon response over the range 0.4–0.7 μm and filters that remove radiation outside this wavelength

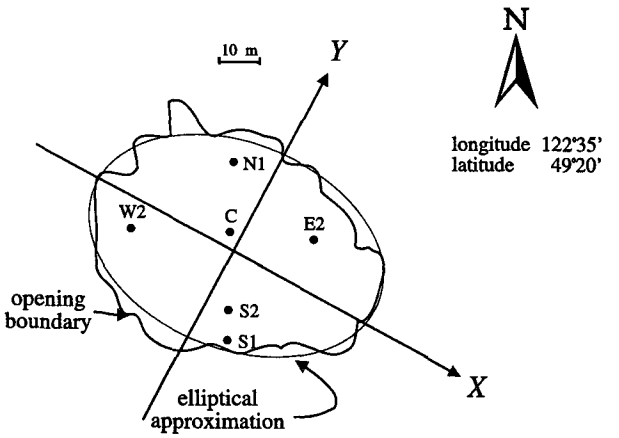

FIG. 5. The experimental layout of the forest opening used to test the model. The boundary of the opening is approximated by an ellipse with a long axis of 82 m and a short axis of 60 m. The long axis X coincides with the line of maximum slope (12°). The average height of the surrounding trees was 38 m. The locations of the six quantum sensors are indicated as C (center), N (north), E (east), W (west), S1 (south 1), and S2 (south 2).

range. The signals from the sensors were recorded continuously using a data logger (Campbell Scientific Inc., Logan, Utah, model 21X) from 25 July to 12 November 1991. The signals were sampled every ten seconds and averaged hourly. To obtain the incident PPFD above the forest stand, a reference site was chosen on the top of a nearby hill (about 150 m from the opening), where another LI-COR quantum sensor and a Moll Gorczynski pyranometer (Kipp and Zonen, Delft, The Netherlands, Model CM5) were mounted and hourly averages obtained over the same period using a separate 21X data logger.

4. Model validation

From the experimental period, a cloudless day (15 August) and an overcast day (7 September) were chosen to validate the model. Figure 6 shows the diurnal variations of the measured total PPFD on these two days at the reference site.

Since the sensors were mounted horizontally close to the sloping ground, comparisons were made between the measured values and those modeled for the case of a horizontal surface just above a slope. Figure 7 compares the measured hourly averages and the modeled total PPFD values for 15 August for six locations in the opening. The modeled values were calculated at 6-min intervals. The total PPFD above the stand obtained from the reference site (Fig. 6) was separated into direct and diffuse components using the following empirical equations (Gates 1980),

$$Q_D = S_0\gamma \cos\theta_r \tau^{1/\cos\theta_r} \quad (40)$$

$$Q_d = S_0\gamma \cos\theta_r (0.271 - 0.294\tau^{1/\cos\theta_r}), \quad (41)$$

where S_0 is the solar constant, taken to be 1373 W m^{-2} (Monteith and Unsworth 1990); γ is the ratio of the PPFD (μmol m^{-2} s^{-1}) to the solar irradiance (W m^{-2}), being 2.02 μmol J^{-1} from our measurements over the entire experimental period including all weather conditions, which is very similar to the value of 2.04 μmol J^{-1} reported by Meek et al. (1984); and τ is the atmospheric transmissivity of the solar beam, for which a value of 0.7 was found to give the best fit to our hourly measurements.

At location C, the center of the opening, measured and modeled values near noon (Fig. 7a) are smaller than those above the stand (Fig. 6) because the diffuse component was reduced by the surrounding trees. The boundary of the opening affected the direct PPFD in the early morning and the late afternoon. At location N close to the north boundary (Fig. 7b), the diurnal variation is similar but the attenuation of the direct PPFD in the afternoon was more significant. Location E was in shade for a large part of the morning but was almost continuously fully exposed to the sun throughout the rest of the day because this location is close to the highest point in the opening (Fig. 7c). As expected, the shading period is reversed at location W (Fig. 7d) and is longer than at location E because it is the lowest point in the opening. The smooth increase in the modeled PPFD in the morning for location E and the smooth decrease in the afternoon for location W indicate that the attenuation of the solar beam is correctly modeled. Location S1 is in shade throughout the day (Fig. 7e) with a low percentage of beam transmission through the canopy. In comparison, the probability of beam transmission to location S2 is much higher (Fig. 7f). The modeled values do not agree with the measured values very well for this location because of the error introduced in approximating the opening boundary with an ellipse. In the morning, the modeled values are larger than the measured values because the

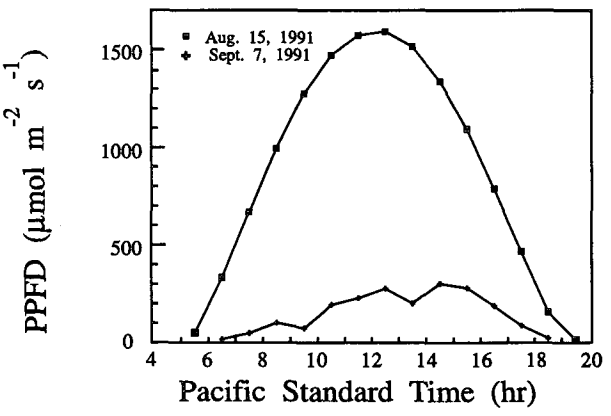

FIG. 6. Total photosynthetic photon flux densities (PPFD) measured on a cloudless day (15 August 1991) and on an overcast day (7 September 1991) on a hill (reference site) near the forest opening shown in Fig. 5.

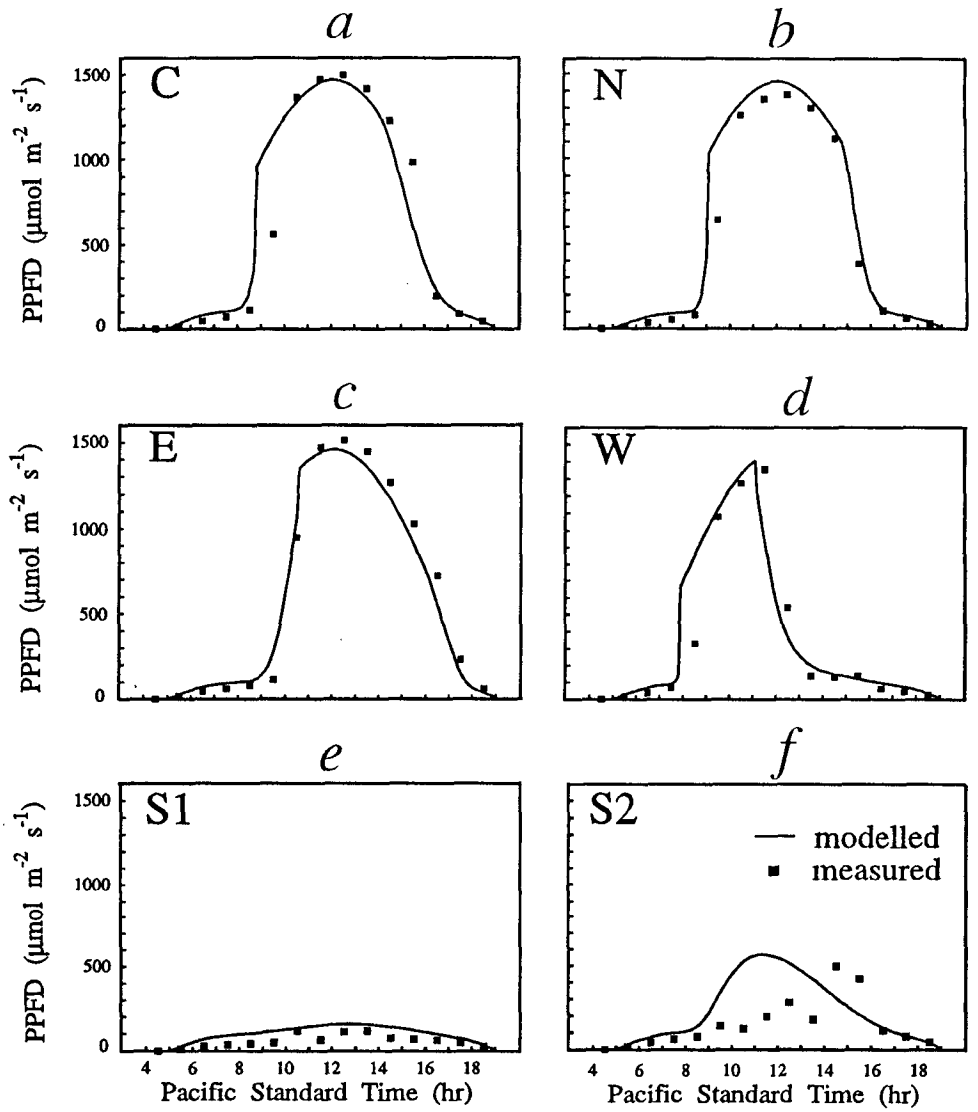

FIG. 7. Comparison of modeled and measured values of PPFD for the cloudless day (15 August 1991) for locations (a) *C*, (b) *N*, (c) *E*, (d) *W*, (e) S1, and (f) S2.

forest edge is farther north than the elliptical curve, and in the afternoon the opposite occurs. Regardless of these discrepancies, it can be seen from all these cases that the model is able to predict the measured values reasonably well with the simple elliptical approximation to the opening boundary. This demonstrates that the equations describing both the opening geometry and the solar trajectory are correct in the model. The root-mean-square error (rmse) and the mean bias error (MBE) of the modeled results for this day are 136 and -40 μmol m^{-2} s^{-1}, respectively. The Willmott *d* (Willmott 1981), which is an index of agreement between modeled and measured values, is 0.989.

The model performance in predicting the diffuse component is shown in Fig. 8 for the overcast day 7 September. The model was run in this case at hourly intervals using the measurements of total PPFD at the reference site, which were considered to be 100% diffuse. The sky view factors were 0.488, 0.365, 0.403, 0.375, 0.364, and 0.431 for the horizontal sensors at the locations *C*, *N*, *E*, *W*, S1, and S2, respectively. The modeled PPFD values compare well with the measured values for all six locations in the opening, with the latter ranging from 48% to 63% of the values above the opening, that is, those observed at the reference site. The reflection of the incident diffuse PAR by the surrounding trees and the transmission and scattering of PAR from the sky through the canopy contributed to the total diffuse PPFD by 12%–17%.

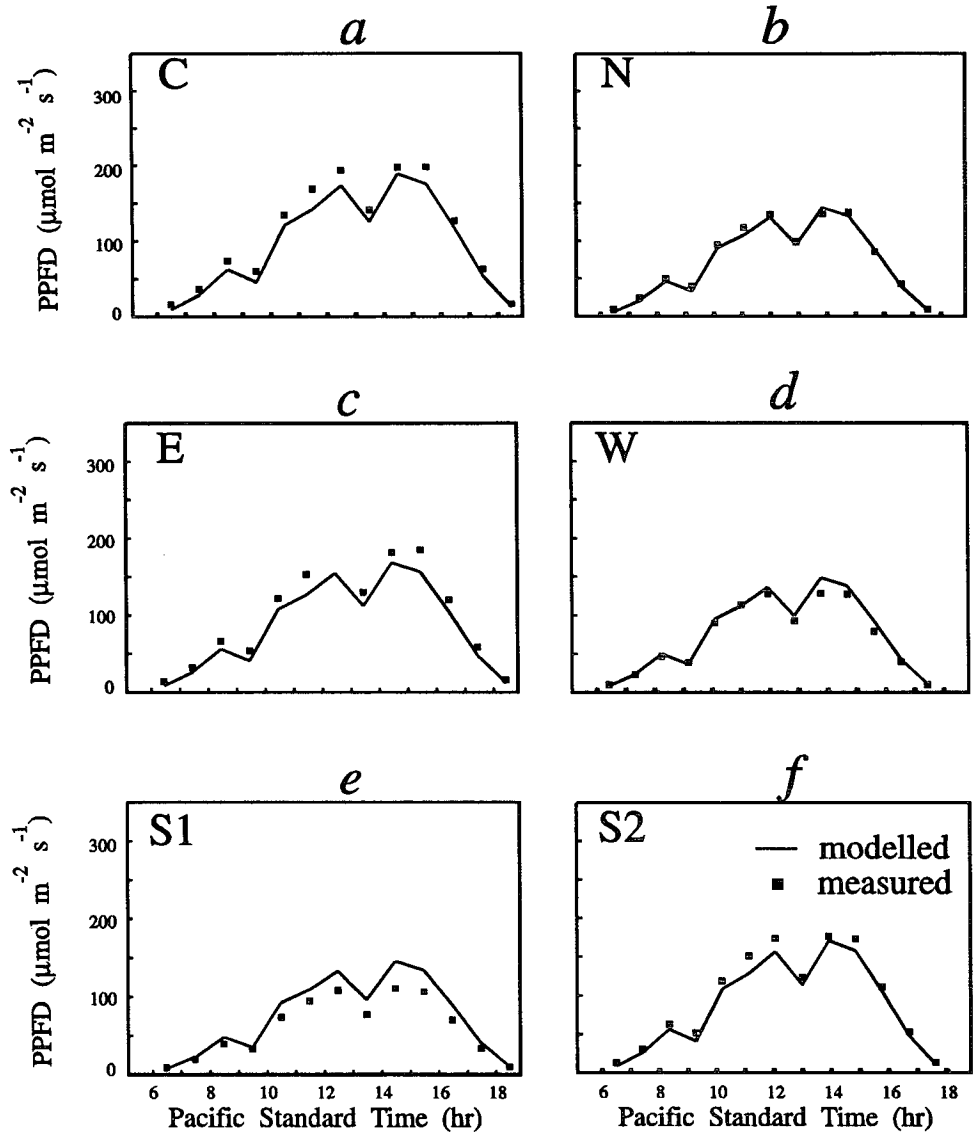

FIG. 8. Comparison of modeled and measured values of PPFD for the overcast day (7 September 1991) for location (a) *C*, (b) *N*, (c) *E*, (d) *W*, (e) S1, and (f) S2.

The model underpredicts the diffuse PPFD for locations *C*, *E*, and S2, but overpredicts for location S1. This is caused by the small error introduced in assuming that the sky radiance is isotropic. The southern portion of the sky seen at locations *C*, *E*, and S2 would have been brighter than the northern portion of the sky seen at location S1. Since this error is small, we do not include in the model an empirical equation reported by Steven and Unsworth (1980) for calculating the distribution of sky radiance under overcast conditions, nor the algorithms obtained by Hooper et al. (1987) for the distribution under clear sky conditions. The rmse and MBE for this day are 12 and 3 μmol m^{-2} s^{-1}, respectively, while the Willmott *d* is 0.996.

5. Conclusions

A computer model has been constructed for calculating direct and diffuse incident photosynthetic photon flux densities at different locations in forest openings of various sizes and shapes on surfaces of various slopes and aspects. Tests of the model were made using field measurements in a 0.37-ha opening in a western hemlock–Douglas fir forest. The model predicted the measured direct and diffuse PPFD very well under cloudless and overcast weather conditions.

The use of an ellipse to describe the boundary of a forest opening has the advantage of being able to represent a wide range of opening shapes with reasonable accuracy and convenience, although this simple geometry may be a limitation when the model is applied to clear-cuts of irregular shapes and polygons with sharp corners.

The various mechanisms contributing to the diffuse irradiance incident on the surface in forest openings are included in the model. This is necessary when considering the levels of PAR required for tree seedling regeneration in small openings. The algorithms developed for calculating the transmission of PAR through the forest edge and the various view factors are useful for estimating other radiation components such as total incident shortwave, longwave, and net all-wave radiation.

Acknowledgments. This research was supported by a contract from B. C. Ministry of Forests, Burnaby, British Columbia. The program is written in Borland Turbo Pascal and is available from the corresponding author.

APPENDIX A

Local Slope

The slope of a surface is defined as the zenith angle of the normal to the surface or the angle between the maximum slope line in the up- or downslope direction and a horizontal line in the same direction, that is, the angle θ_s in Fig. A1. The slope in other directions would change from θ_s. Figure A1 illustrates how the slope $\theta_{s\beta}$ in a given direction β relates to the maximum slope θ_s. Because

$$\tan\theta_s = \frac{\overline{AB}}{\overline{OB}} \tag{A1}$$

$$\tan\theta_{s\beta} = \frac{\overline{CD}}{\overline{OD}} \tag{A2}$$

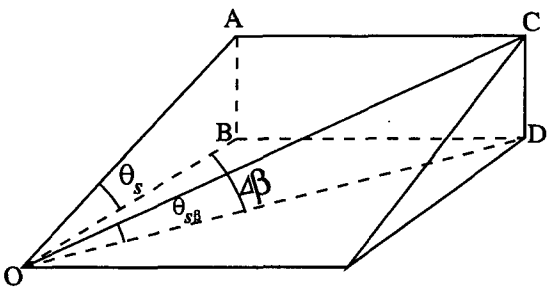

FIG. A1. Maximum slope θ_s and the slope $\theta_{s\beta}$ in the direction β; $\Delta\beta$ is the difference between the direction of maximum slope (β_s) and the direction β.

and

$$\overline{AB} = \overline{CD} \tag{A3}$$

$$\overline{OD} = \frac{\overline{OB}}{\cos(\beta - \beta_s)} \tag{A4}$$

it can be shown that

$$\theta_{s\beta} = \arctan[\tan\theta_s \cos(\beta - \beta_s)], \tag{A5}$$

where β_s is the direction of the maximum slope. This is Eq. (12); $\theta_{s\beta}$ varies from $-\theta_s$ in the downslope direction to θ_s in the upslope direction. When $\pi/2 < (\beta - \beta_s) < 3\pi/2$, that is, β is in the downslope direction, $\theta_{s\beta}$ is negative.

APPENDIX B

Pathlength through the Forest Canopy

This appendix shows how the path $\overline{AB}$ and the exit height h in Fig. 4 are derived from the known parameters: the local slope $\theta_{s\beta}$, the solar zenith angle θ_r, the tree height H, and the distance D_2 [calculated in Eq. (16)]. The angles in the triangle OBC are given as follows:

$$\angle OBC = \theta_r \tag{B1}$$

$$\angle OCB = \frac{\pi}{2} - \theta_{s\beta} \tag{B2}$$

$$\angle BOC = \frac{\pi}{2} - (\theta_r - \theta_\beta). \tag{B3}$$

From the sine theorem, we can write that

$$\overline{OB} = \frac{\overline{OC}\sin\angle OCB}{\sin\angle OBC} = \frac{D_2\cos\theta_{s\beta}}{\sin\theta_r}. \tag{B4}$$

From the similarity between the triangles OBC and OAD and the sine theorem, we have

$$\overline{OA} = H\frac{\overline{OB}}{\overline{BC}} = H\frac{\sin\angle OCB}{\sin\angle BOC} = H\frac{\cos\theta_{s\beta}}{\cos(\theta_r + \theta_{s\beta})}. \tag{B5}$$

Since $\overline{AB} = \overline{OA} - \overline{OB}$, it can be shown from Eqs. (B4) and (B5) that

$$\overline{AB} = \cos\theta_{s\beta}\left[\frac{H}{\cos(\theta_r + \theta_{s\beta})} - \frac{D_2}{\sin\theta_r}\right]. \tag{B6}$$

Although Eq. (B6) is derived for the case that the incident solar beam is from the upslope direction, it can be used for calculating the pathlength in the downslope direction with D_2 replaced with D_1. $\theta_{s\beta}$ will be negative for the downslope direction (appendix A).

From the sine theorem, the exit height h can be shown to be

$$h = \frac{D_2\cos(\theta_r + \theta_{s\beta})}{\sin\theta_r}. \tag{B7}$$

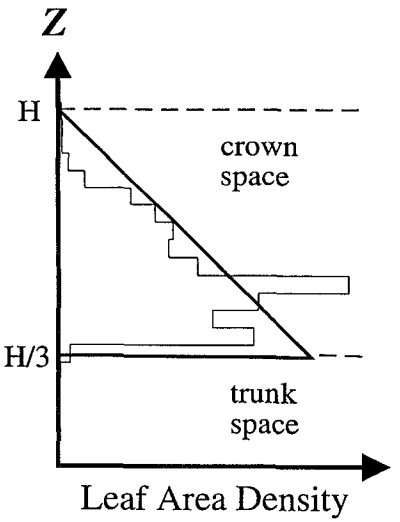

FIG. C1. Linear distribution of the leaf area density with height. Also shown is the measured distribution in a 20-year-old Douglas fir stand that was thinned and pruned two years before the measurements.

APPENDIX C

Leaf Area Index

Figure C1 shows the assumed linear distribution of leaf area density $[a(z)]$ given by

$$a(z) = \begin{cases} C(H - z), & z \geqslant H_0 \\ 0, & z < H_0, \end{cases} \quad \text{(C1)}$$

where $H_0 = H/3$. Given that the leaf area index of the stand (L) is known, the coefficient C in Eq. (C1) can be found from the following integration:

$$L = \int_0^H a(z)dz = \frac{C}{2}(H - H_0)^2. \quad \text{(C2)}$$

The leaf area index accumulated downward in the vertical direction to the exit height h is obtained from

$$L_h = \int_h^H a(z)dz = \frac{C}{2}(H - h)^2 = L\frac{(H - h)^2}{(H - H_0)^2}. \quad \text{(C3)}$$

If $h < H_0$, then $L_h = L$.

The leaf area index accumulated in the direction of the solar beam and over the path $\overline{AB}$ is given by

$$L_{hp} = L_h\frac{\overline{AB}}{(H - h)} = L\frac{\overline{AB}(H - h)}{(H - H_0)^2}. \quad \text{(C4)}$$

REFERENCES

Black, T. A., J. M. Chen, X. Lee, and R. Sagar, 1991: Characteristics of shortwave and longwave irradiances under a Douglas-fir forest stand. *Canadian J. Forest Res.*, **21,** 1020–1028.

Chen, J. M., and T. A. Black, 1991: Measuring leaf area index of plant canopies with branch architecture. *Agric. For. Meteorol.*, **57,** 1–12.

——, ——, 1992: Foliage area and architecture of plant canopies from sunfleck size distributions. *Agric. For. Meteorol.*, **60,** 249–266.

——, ——, and R. S. Adams, 1991: Evaluation of hemispherical photography for determining plant area index and geometry of a forest stand. *Agric. For. Meteorol.*, **56,** 129–143.

Gates, D. M., 1980: *Biophysical Ecology.* Springer-Verlag, 611 pp.

Geiger, R., 1966: *The Climate near the Ground.* Harvard University Press, 611 pp.

Harrington, J. B., 1984: Solar radiation in a clear-cut strip—A computer algorithm. *Agric. For. Meteorol.* **33,** 23–39.

Holbo, H. R., and S. W. Childs, 1987: Summertime radiation balances of clearcut and shelterwood slopes in southwest Oregon. *For. Sci.* **33,** 504–516.

Hooper, F. C., A. P. Brunger, and C. S. Chan, 1987: A clear sky model of diffuse sky radiance. *ASME J. Solar Energy Engineering,* **109,** 9–14.

Howell, J. R., 1982: *A Catalog of Radiation Configuration Factors.* McGraw-Hill Book Company, 243 pp.

Jarvis, P. G., G. B. James, and J. J. Landsberg, 1976: Coniferous forest. *Vegetation and the Atmosphere.* Vol. 2. J. L. Monteith, Ed., Academic Press, 171–240.

Meek, D. W., J. L. Hatfield, T. A. Howell, S. B. Idso, and R. J. Reginato, 1984: A generalized relationship between photosynthetically active radiation and solar radiation. *Agron. J.* **76,** 939–945.

Monteith, J. L., and M. H. Unsworth, 1990: *Principles of Environmental Physics,* Edward Arnold, 291 pp.

Steven, M. D., and M. H. Unsworth, 1980: The angular distribution and interception of diffuse solar radiation below overcast skies. *Quart. J. Roy. Meteor. Soc.,* **106,** 57–61.

Willmott, C. J., 1981: On the validation of models. *Phys. Geogr.,* **2,** 84–194.